JOURNAL OF Applied Polymer SCIENCE

Gold Deposition on Fe_3O_4/(*co*)Poly(*N*-octadecyl methacrylate) Hybrid Particles to Obtain Nanocomposites with Ternary Intrinsic Features

Yuzhen Yang,[1,2] Ali Reza Mahdavian,[3] Eric S. Daniels,[1] Andrew Klein,[1,2] Mohamed S. El-Aasser[1,2]

[1]Emulsion Polymers Institute, Lehigh University, Bethlehem, Pennsylvania 18015

[2]Department of Chemical Engineering, Lehigh University, Bethlehem, Pennsylvania 18015

[3]Polymer Science Department, Iran Polymer & Petrochemical Institute, Tehran 14967, Iran

Correspondence to: E. S. Daniels (E-mail: eric.daniels@lehigh.edu)

ABSTRACT: Here, nanocomposite particles with three domains including magnetite nanoparticles, poly(*N*-octadecyl methacrylate) (PODMA) or poly(*N*-octadecyl methacrylate-*co*-1-vinylimidazole) (P(ODMA-*co*-VIMZ)), and gold nanoparticles were prepared. Fe_3O_4 nanoparticles with narrow particle size distribution were prepared through a synthetic route in an organic phase in order to achieve good control of the size and size distribution and prevent their aggregation during their preparation. These magnetite nanoparticles, $\sim$ 5 nm in size, were then encapsulated and well-dispersed in PODMA and P(ODMA-*co*-VIMZ) matrices via a miniemulsion polymerization process to obtain the corresponding nanocomposite particles. The results revealed that Fe_3O_4 nanoparticles were encapsulated and did not migrate towards the monomer/water interface during polymerization. The resulting latex was used as a precursor for the adsorption of Au^{3+} ions on the surface of the polymeric particles and subsequent reduction to produce Fe_3O_4/P(ODMA-*co*-VIMZ)/Au nanocomposite particles. The morphology of the particles from each step was fully characterized by TEM and AFM, and the results of DLS analysis showed their size and size distribution. Measurement of magnetic properties illustrated the superparamagnetic characteristic of the products and it was observed that the encapsulation process and deposition of gold had no effect on the magnetic properties of the resulting particles. © 2012 Wiley Periodicals, Inc. J. Appl. Polym. Sci. 000: 000–000, 2012

KEYWORDS: nanoparticles; magnetite; gold; acrylic; miniemulsion polymerization

Received 9 January 2012; accepted 7 March 2012; published online 00 Month 2012

DOI: 10.1002/app.37647

INTRODUCTION

Magnetic nanocomposite particles have recently received considerable attention because of their potential applications in the electronic and biomedical fields. These particles can be applied to magnetic data storage, and the future development of high-density magnetic storage media will be based heavily on stable magnetic materials, which are just few nanometers in size.[1] Among these magnetic nanoparticles, magnetic iron oxides, and in particular, magnetite (Fe_3O_4) nanoparticles, are attractive because of their high magnetic moment, nontoxic nature, and ease of synthesis.[2] Several applications in which the magnetic properties of Fe_3O_4 are envisaged include ferro fluids for magnetic separation science and technology,[3–5] biomedical applications and cancer treatment,[6,7]magnetic resonance imaging,[8,9] targeted drug delivery,[10–12] and gene therapy.[13,14] Magnetic properties of the produced magnetite are quite important and improve its utility, specifically in biological systems. Therefore, the preparation of superparamagnetic Fe_3O_4 has been a main topic of interest in recent years.[15] In addition to their magnetic properties, the biomedical applicability of nanoscale magnetite particles is dependent upon their stability against aggregation in physiochemical environments, and proper functionalization of the particle surface is needed for specific biomolecule interactions.[16] Stability against aggregation is particularly important for *in vivo* applications in which this aggregation would cause unwanted accumulation of particles or blood vessel blockage at natural pH.[17] These issues have led to the modification of magnetite with various inorganic materials such as silica,[18] gold,[19–21] and several organic substances such as dextrane,[22] polyethylene glycol,[23,24]and polyvinyl alcohol.[25] Future developments in this area will rely primarily on magnetite particles, which are only a few nanometers in size. Hence, a practical route to prepare monodisperse Fe_3O_4 nanoparticles smaller than 20 nm and with a narrow size distribution is needed. A commonly used solution-phase procedure for preparing such particles is the coprecipitation of Fe^{2+} and Fe^{3+} ions in the

TABLE I Synthesis of PODMA, Fe_3O_4/PODMA, and Fe_3O_4/P(ODMA-*co*-VIMZ) Latexes Via Miniemulsion Polymerization[a]

Ingredient	PODMA	Fe_3O_4/PODMA	Fe_3O_4/P(ODMA-*co*-VIMZ)	Comments
ODMA (g)	5	5	5	10 wt % based on total amount of latex
VIMZ (g)	–	–	0.5	10 wt % based on ODMA amount
Fe_3O_4 (g)	–	0.05–0.5	0.055–0.55	1–10 wt % based on total monomer amount
AIBN (mg)	15	15	15	1 mmol
Hexadecane (g)	0.2	0.2	0.2	4 wt % based on monomer
CTAB (g)	0.36	0.36	0.36	20 m*M* based on water phase
$NaHCO_3$ (g)	0.1	0.1	0.1	
DI water (g)	45	45	45	90 wt % based on total amount of latex

*Polymerization was run at 70°C for 24 h.

presence of a base, usually NaOH or NH_3 in an aqueous solution[26,27]or in a reverse micelle template.[28,29] Although, the precipitation technique has several advantages, it still requires careful adjustment of pH of the solution for particle formation and stabilization. In addition, particle size control and obtaining a narrow size distribution are serious problems especially for those particles smaller than 20 nm.[30] Another approach for the preparation of monodisperse Fe_3O_4 is through organic phase decomposition of some iron precursors at high temperatures and thermal treatment.[31–33] Sun et al. have reported a convenient organic phase process for the preparation of monodisperse Fe_3O_4 nanoparticles via a redox reaction.[34] This technique has the great advantage of preparing nanoparticles with tunable sizes from 3 to 20 nm and narrow particle size distributions, while at the same time overcoming aggregation of the nanoparticles in the aqueous phase during the preparation process.

Gold represents an excellent candidate for biomedical research by virtue of its easy reductive preparation, high chemical stability, biocompatibility, and its affinity for binding to amine/thiol terminal groups of organic molecules.[35] Composite particles containing both magnetite and gold have become increasingly important recently as both magnetic and plasmonic properties come together in a single particle.[36,37] Methods for the coating of gold on the surface of magnetite can be categorized based on the reaction media. The first method is the synthesis and coating in the aqueous phase.[15,38] The aqueous methods are simple and quick, but the aggregation of magnetite and control of the gold-shell deposition are problematic. The second method consists of magnetite synthesis and gold coating in an organic phase.[35,39] Organic methods usually result in significantly enhanced particle size and shell thickness control with excellent resistance to aggregation in the organic solvent. The main concern would be the occurrence of aggregation when the phase is transferred into the aqueous environment. To achieve size control and effectiveness in the water phase, a third method of synthesis has emerged more recently, involving a combination of the organic phase synthesis of magnetite followed by coating with the gold in an aqueous phase.[21,40] In another approach, reverse micelle methods are able to form gold-coated particles, but are of low yield and are fairly difficult to reproduce.[41]

In this work, we prepared nanocomposite particles via the aforementioned third method and exploited a biocompatible polymeric interface between the magnetite core and the outer gold shell. The steric stability resulting from the presence of the polymeric shell between the magnetite core and the outer gold particles will be responsible for the prevention of aggregation of the primary-produced magnetite nanoparticles while maintaining their size distribution and magnetic properties. Also, the polymeric shell would be a reservoir for the loading of oil-soluble drugs that can potentially be used for targeted drug delivery systems. This approach is quite novel and there are only a few reports on the preparation of such particles. For example, Goon et al. utilized poly(ethyleneimine) for the dual function of attaching gold seeds and preventing the formation of large aggregates through the aqueous synthetic method.[2] In a recent attempt, gold has been decorated on the surface of Fe_3O_4/polystyrene particles, coated with poly(methyl methacrylate).[42] Hsiao et al's strategy was to prepare magnetite nanoparticles using a hydrothermal method, utilizing the suspension polymerization of styrene in the presence of Fe_3O_4, followed by the seeded growth emulsifier-free emulsion polymerization of methyl methacrylate including Fe_3O_4/polystyrene and finally, self-reduction for deposition of gold on the outer layer of the particles.

To achieve the encapsulation of inorganic particles into the polymeric matrix, several methods have been developed, including emulsion-based techniques. Considering the mechanism of different emulsion systems, miniemulsion polymerization[43,44] has been proven to be a promising methodology for the encapsulation of inorganic particles,[45–48] and more specifically it was

Table II. Preparation of Fe_3O_4/P(ODMA-*co*-VIMZ)/Au Nanocomposite Particles

Ingredient	MCG1	MCG2
Fe_3O_4/P(ODMA-*co*-VIMZ) latex (solids content = 10–11%)	5 g	5 g
$HAuCl_4$ solution (0.4 g/L)	3 g	6 g
$[Au^{3+}]$	0.454 m*M*	0.908 m*M*
$NaBH_4$ solution (0.1177*M*)	0.03 mL	0.03 mL

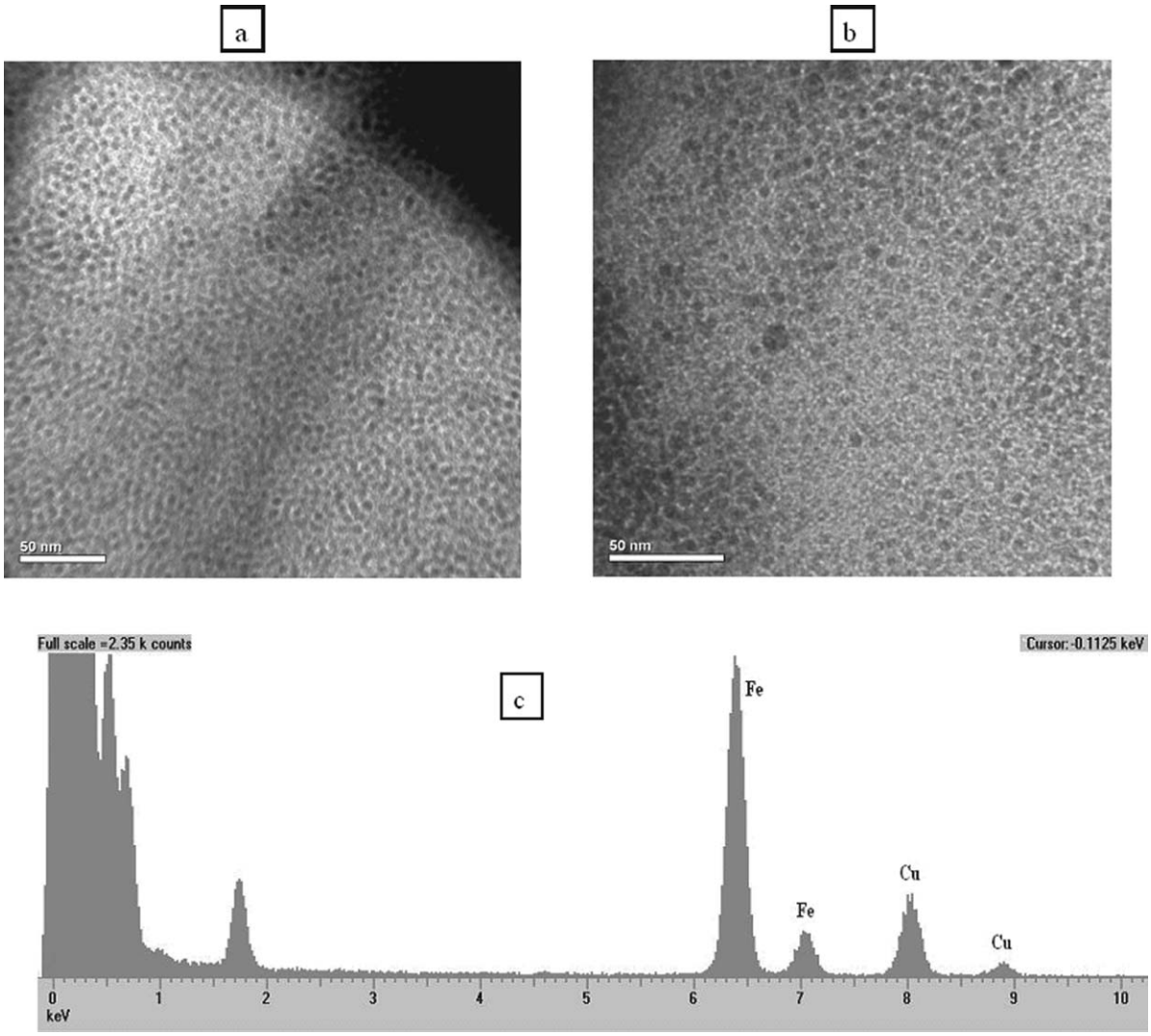

Figure 1. (a, b) TEM images and (c) EDS analysis of the synthesized Fe_3O_4 nanoparticles (Cu peaks appear due to the scattering caused by the copper grid for TEM analysis.

recently used for magnetite nanoparticles.[49,50] In a miniemulsion polymerization,[44,51] each of the submicrometer monomer droplets is the main site for particle nucleation and growth[52] and as such may be regarded as an individual nanophase reactor.[43,53] The characteristic features of the miniemulsion polymerization technique would offer potential advantages in controlling the particle size, allowing for direct dispersion of the hydrophobic inorganic particles in the monomer phase, the possibility of nucleating the majority of droplets containing inorganic particles, and faster polymerization rate.[44,46,47,54]

To the best of our knowledge, there are no reports on the application of miniemulsion polymerization as an effective technique for the preparation of nanocomposite particles with three domains, by the encapsulation of well-dispersed magnetite nanoparticles in the monomeric phase followed by the miniemulsification and then polymerization of the miniemulsion monomer droplets, and the subsequent decoration of the particle surface with gold nanoparticles. Here, we have exploited this method for copolymerization of *N*-octadecyl methacrylate (ODMA) and 1-vinylimidazole (VIMZ) on the surface of Fe_3O_4 nanoparticles. Then Au nanoparticles were surface-adsorbed and grown through the aqueous phase reduction of $HAuCl_4$, which results in the formation of nanocomposite particles with triple distinct domains.

EXPERIMENTAL

Materials

Iron (III) acetylacetonate ($Fe(acac)_3$) (Strem Chemicals, MA), 1,2-hexadecanediol (Sigma-Aldrich, MO), oleic acid (Spectrum Chemical, CA), oleylamine (TCI, OR), diphenyl ether (Alfa Aesar, MA), and hexane (Alfa Aesar) were used without further purification. ODMA (Sigma-Aldrich) and VIMZ (Sigma-Aldrich, MO) were purified by passing the monomer through an inhibitor-removal column (Sigma-Aldrich, MO). 2,2′-azobis(isobutyronitrile) (AIBN) (Sigma-Aldrich, MO) was used as initiator. Cetyl trimethyl ammonium bromide (CTAB) (Sigma-Aldrich, MO) as surfactant and hexadecane (HD) (Acros Organics, NJ) as costabilizer were applied. Sodium bicarbonate

Applied Polymer SCIENCE

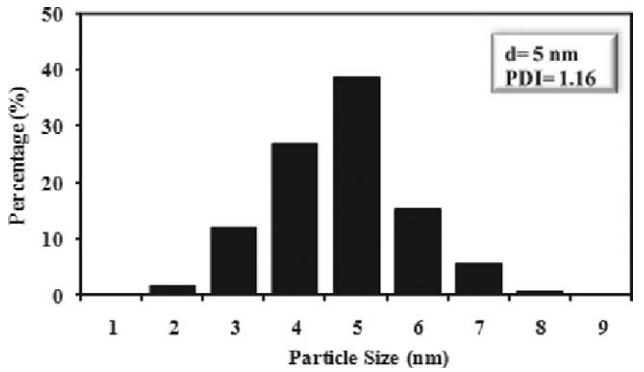

Figure 2. Particle size distribution of the prepared Fe_3O_4 nanoparticles.

(Mallinckrodt Chemicals, NJ) was employed as a buffer and phosphotungstic acid (PTA) (Fisher Scientific, NJ) was utilized for negative staining under TEM. Gold (III) chloride hydrate ($HAuCl_4$) 99.9%, (Sigma-Aldrich, MO) and sodium borohydride ($NaBH_4$) (Sigma-Aldrich, NJ) were used for the gold encapsulation process. Deionized (DI) water was used in all experiments.

Characterization

Latexes were diluted with deionized water and their particle size and size distribution were measured by dynamic light scattering (DLS, Nicomp, Model 370). Fe_3O_4 nanoparticles, poly(ODMA) (PODMA) latex particles and all other nanocomposite particles were imaged by transmission electron microscopy (TEM, Jeol 2000, 200 KV, Japan) and atomic force microscopy (AFM, Veero Dimension 5, Digital Instruments, NY). For the TEM and EDS analysis, a negative staining technique was applied to obtain high quality results. 10 drops of 2 wt % PTA was added into PODMA latex (1 wt % solids) with dilution prior to drying on the copper grid. Then the samples were dried at room temperature for 24 h. Elemental analysis of magnetic nanocomposite particles was recorded by energy dispersive spectrometry (EDS, Jeol 2000, Japan). AFM samples were prepared by drying one drop of diluted polymer latex on the surface of a precleaned glass slide for 24 h at ambient conditions. The verification of magnetic particles was performed via wide angle X-ray diffraction (XRD, Rigaku, Tokyo, Japan). Magnetic properties were measured by vibrating sample magnetometer (VSM, Model 3900-04, Princeton Measurements Corporation, NJ). Also, the

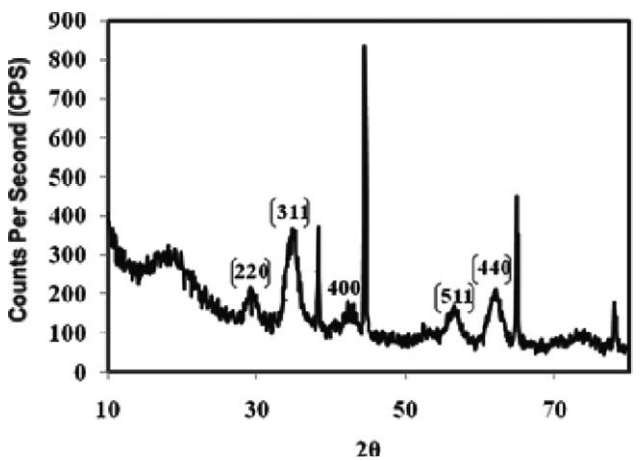

Figure 3. Wide-angle XRD analysis of the prepared Fe_3O_4 nanoparticles.

Table III. Particle Diameters and Size Distribution of PODMA Particles at Different CTAB Concentrations

CTAB conc. (mM)	D_W (nm)	D_V (nm)	D_N (nm)	PDI
15	256	253	234	1.09
20	231	226	210	1.10
40	322	327	312	1.03

D_W is weight-average diameter, D_V is volume-average diameter, D_N is number-average diameter, and PDI is polydispersity index (D_V/D_N).

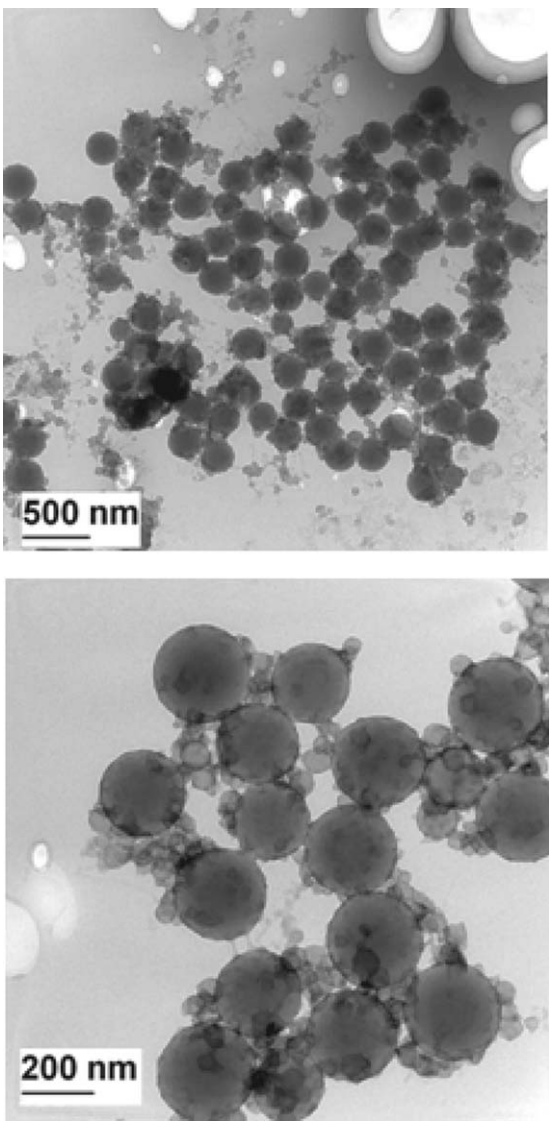

Figure 4. TEM micrographs of PODMA particles stained with PTA; darker and larger particles are PODMA and smaller and brighter (disordered) ones represent the added PTA.

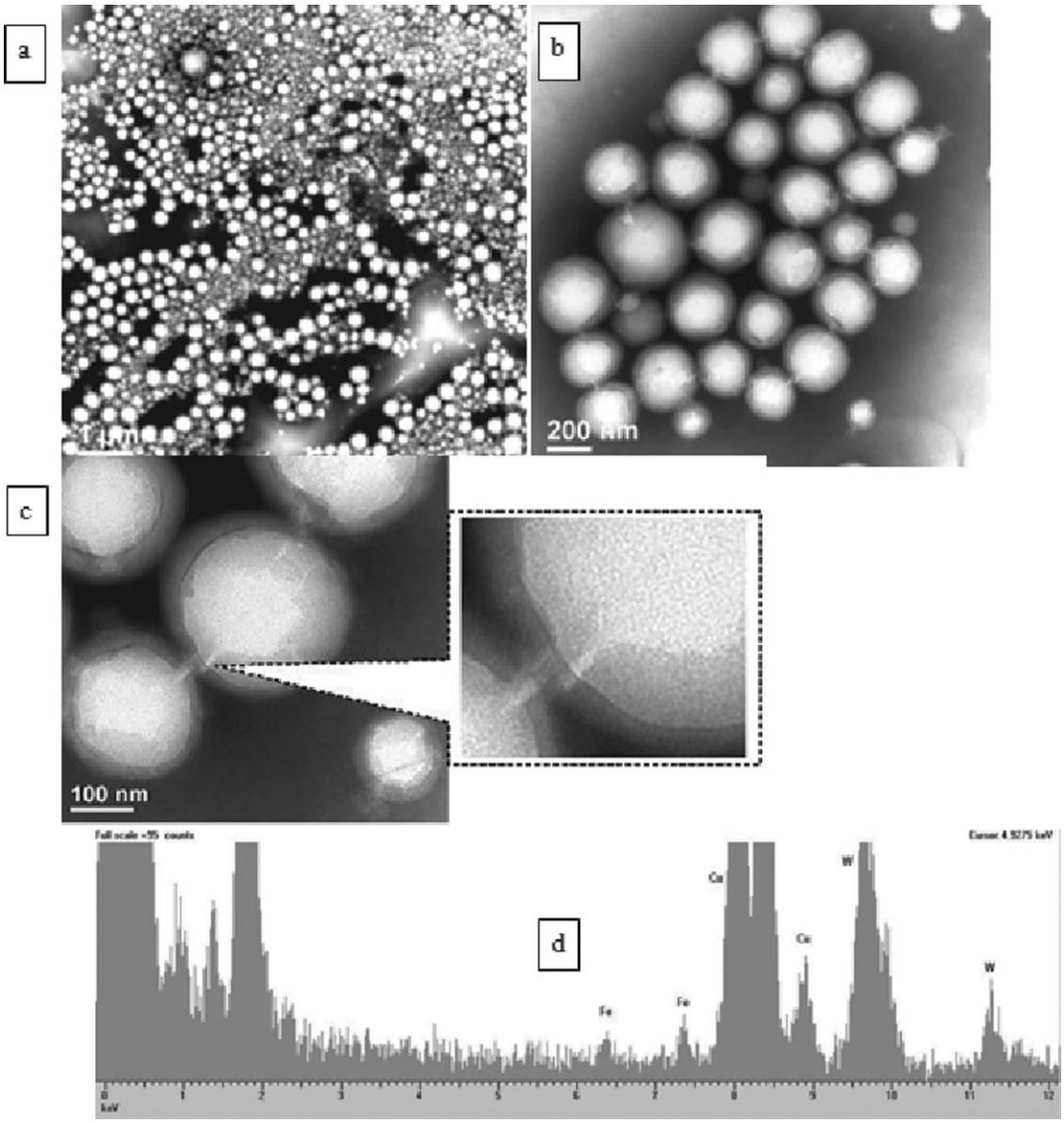

Figure 5. (a–c) TEM images at different magnifications, and (d) EDS analysis of Fe_3O_4/PODMA nanocomposite particles (W peaks are related to the presence of phosphotungstic acid used for the preparation of the stained sample, and Cu peaks appear because of scattering caused by the copper grid for TEM analysis).

conversion of monomers during the polymerization process was determined gravimetrically.

Preparation of Magnetite Nanoparticles in the Oil Phase

Magnetic nanoparticles were prepared in diphenyl ether according to a previously reported procedure.[34] 0.71 g (2 mmol) $Fe(acac)_3$, 2.58 g (10 mmol) 1,2-hexadecanediol, 1.69 g (6 mmol) oleic acid, and 1.60 g (6 mmol) oleylamine were immersed in 21.46 g (20 mL) diphenyl ether and the reaction mixture was heated to 200°C and kept at that temperature for 30 min. Then the mixture was heated to reflux conditions at 265°C for another 30 min under a blanket of nitrogen. The black–brown mixture was then cooled to room temperature and the prepared Fe_3O_4 nanoparticles were centrifuged three times at 5000 rpm and redispersed in hexane. Hexane was then removed at ambient temperature and the resulting magnetite nanoparticles were redispersed in the monomeric oil phase.

Miniemulsion Polymerization

Miniemulsion polymerization using AIBN as initiator was carried out via a batch polymerization process.[47,51] The recipes used for the synthesis of PODMA and encapsulated Fe_3O_4 into PODMA (Fe_3O_4/PODMA) and poly(ODMA-*co*-VIMZ) (Fe_3O_4/P(ODMA-*co*-VIMZ) are listed in Table I.

The aqueous phase and oil phase were prepared separately. Then the oil phase was slowly added into the aqueous phase in a 100 mL beaker while stirring using a magnetic bar. The crude emulsion was then sonified using a sonifier (Bronson W450, ½

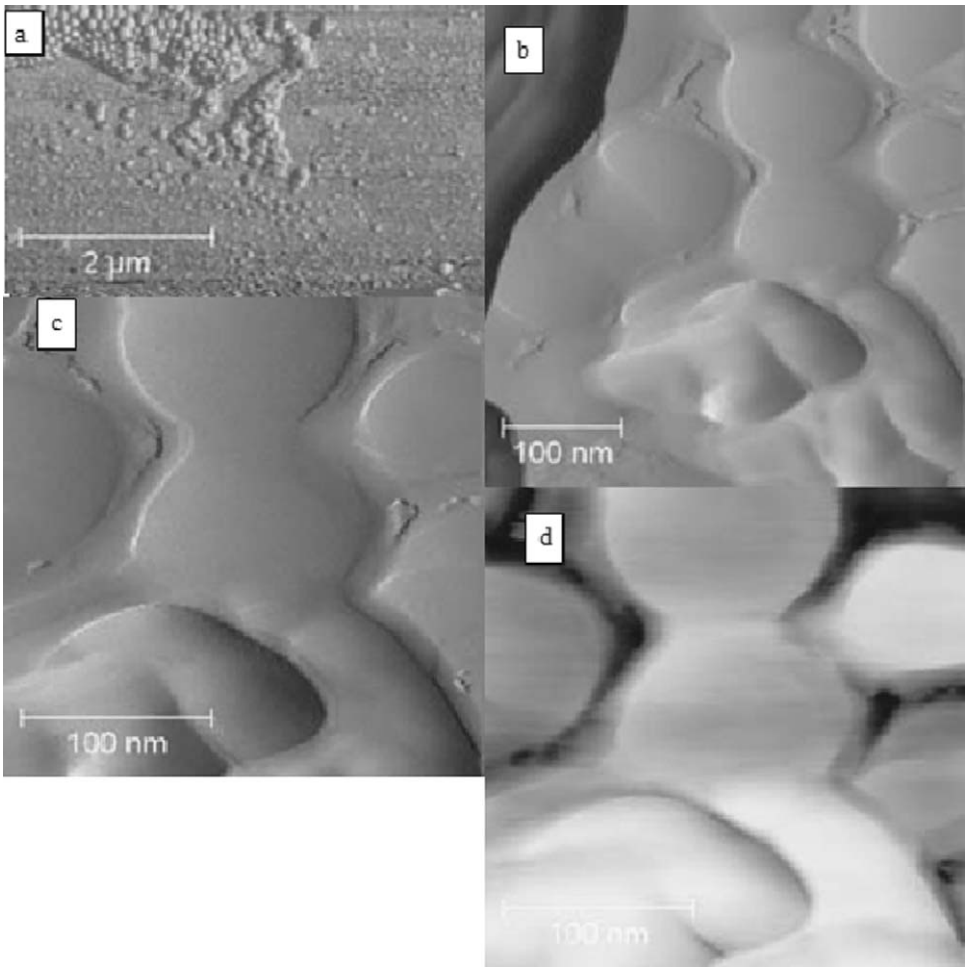

Figure 6. (a–c) AFM micrograph of Fe_3O_4/PODMA nanocomposite particles with different magnifications, (d) represents the phase profile of the same position for (c).

inch Tip, Branson Ultrasonics, CT) at a power level of 8 and 50% duty cycle for 30 s. The miniemulsion was then transferred into a 2 oz (56 mL) glass bottle, which was then purged with nitrogen, capped, and sealed. The bottles were then placed in a bottle polymerization unit and tumbled end-over-end at 40 rpm at 70°C for 24 h. The encapsulation of Fe_3O_4 nanoparticles into polymeric particles followed the same procedure as above, besides adding 1–10 wt % of Fe_3O_4 nanoparticles (based on monomer quantity) into the oil phase.

Deposition of Gold on the Surface of Fe_3O_4/P (ODMA-*co*-VIMZ) Particles

Deposition of Au on the surface of Fe_3O_4/P(ODMA-*co*-VIMZ) particles was carried out by utilizing a metal–ligand formation approach[55] according to the recipe given in Table II. $HAuCl_4$ (0.4 g/L) aqueous stock solution was used as the source of the Au^{3+} ions. After preparation of Fe_3O_4/P(ODMA-*co*-VIMZ) nanocomposite particles with 10 wt % magnetite, 3 g of $HAuCl_4$ stock solution was added to 5 g of the preformed latex with stirring for 24 h at room temperature. The reduction of Au^{3+} ions that were chelated to the VIMZ on the surface of the Fe_3O_4/P(ODMA-*co*-VIMZ) particles were carried out by adding 0.03 mL $NaBH_4$ stock solution to 8 g of the Au^{3+}-associated latex at room temperature to give nanocomposite particles with three domains (Fe_3O_4/P(ODMA-*co*-VIMZ)/Au). The $NaBH_4$ stock solutions were freshly prepared at a concentration of 0.1177*M*.

RESULTS AND DISCUSSION

Synthesis of Magnetite Nanoparticles

Preparation of Fe_3O_4 nanoparticles was performed in diphenyl ether as an organic media according to the procedure because of its efficiency in excluding the possibility of aggregation of these nanoparticles that is a serious concern in the aqueous phase. TEM images and elemental analysis of the resulting magnetite nanoparticles are shown in Figure 1.

Total yield of this recipe was about 97%, which was measured gravimetrically. From Figure 1, it could be found that the size of Fe_3O_4 nanoparticles is around 5 nm and the polydispersity (PDI) is quite narrow. To confirm the composition of the particles, EDS spectrum [Figure 1(c)] was collected from TEM analysis, confirming the presence of Fe ($k_\alpha = 6.4$ and $k_\beta = 7.1$ KeV) in the nanoparticles. The actual particle size was measured

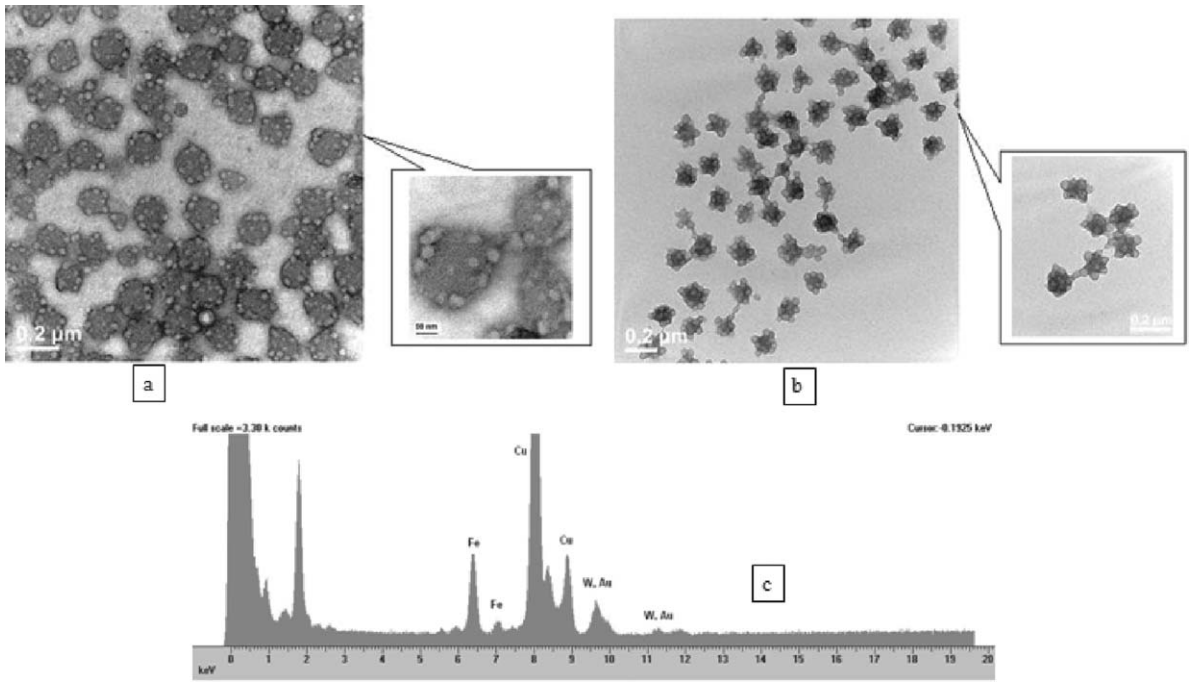

Figure 7. (a) TEM images of MCG1, (b) MCG2, and (c) EDS analysis of Fe_3O_4/PODMA/Au nanocomposite particles (W peaks are related to the presence of phosphotungstic acid used for the preparation of stained samples, and Cu peaks appear due to the scattering caused by the copper grid for TEM analysis.

based on at least 500 particles and their size distribution (PDI is 1.16) is given in Figure 2.

The structure of magnetic nanoparticles was also verified by XRD analysis (Figure 3). The XRD pattern of Fe_3O_4 nanoparticles shows 8 main peaks at 2θ of 19°, 30°, 35°, 42°, 53°, 56°, 62°, and 71° relating to [111], [220], [311], [400], [422], [511], [440], and [533] Bragg reflections, respectively. These peaks and corresponding d values ($2d = \lambda \sin \theta$) confirm the inverse cubic spinal phase of the synthesized Fe_3O_4 crystalline structure.[56] The peaks in the XRD pattern of the resulting nanoparticles (Figure 3) match very well with the standard magnetite (Fe_3O_4) crystal structure data (Joint Committee for Powder Diffraction Studies, JCPDS, Card No. 19-0629). Thus, it could be concluded that Fe_3O_4 nanoparticles with particle size of 5 nm and narrow size distribution were successfully prepared in the oil phase.

Encapsulation of Fe_3O_4 Nanoparticles into Polymeric Particles

To optimize the encapsulation efficiency of Fe_3O_4 nanoparticles into polymeric particles, ODMA was chosen as the monomer for miniemulsion polymerization. It is noteworthy that ODMA is highly hydrophobic and insoluble in water.[57,58] Hence, the probability for incorporation of ODMA and its corresponding polymer (PODMA) into biologically-active material would be negligible and may be considered as a potential bio-inactive material, although no FDA approval yet exists for them.

At first, pure PODMA polymer particles were prepared using AIBN as the oil-soluble initiator based on the recipe shown in Table I. Different concentrations of the cationic surfactant (CTAB) were evaluated in order to optimize the condition for obtaining uniform PODMA particles. The particle sizes as well as their size distribution were measured by DLS and are listed in Table III. The conversion for PODMA polymer particles was about 98 wt % and there was no coagulum at the end of miniemulsion polymerization.

It could be observed that the average size of PODMA particles was 231 nm, when using 20 mM of CTAB with a polydispersity index of 1.1, indicating a narrow particle size distribution. Therefore, the procedure with 20 mM surfactant concentration that resulted in the smallest particle size and reasonable PDI was used in our further investigations. Because of the low T_g of PODMA (about −100°C),[59] a negative staining technique was applied to avoid film formation of PODMA particles during sample preparation and running TEM analysis. TEM images of PODMA polymer particles are shown in Figure 4. However, it should be noted that the particle size as determined by TEM is smaller than the size determined by DLS. The size determined by TEM may not be representative of the actual particle size of the PODMA and nanocomposite particles since only a limited number of TEM micrographs were taken and typically several thousand particles need to be measured to calculate the volume-average particle diameter. If one is able to analyze ∼ 2000 particles from the TEM micrographs from the same sample and calculate the weight and volume particle diameters, then the TEM and DLS average diameters should be close to one another.

Fe_3O_4 nanoparticles (5 nm in size) were encapsulated into PODMA particles via the above optimized miniemulsion

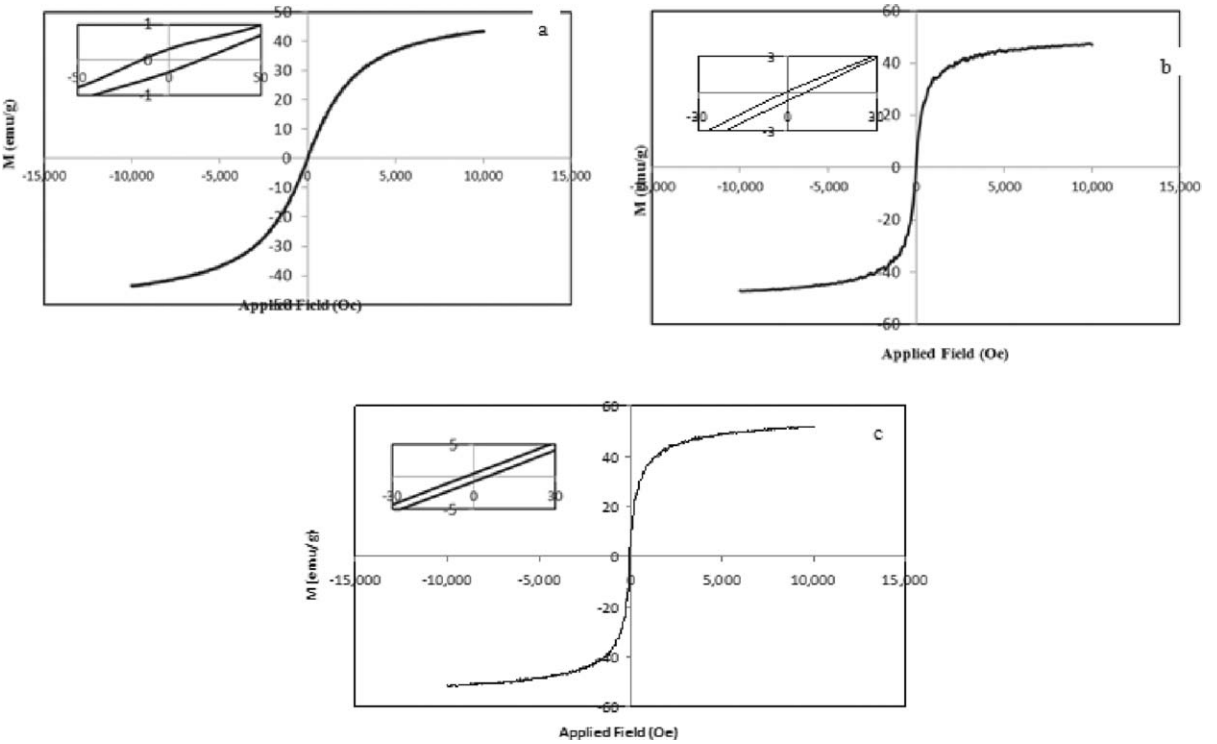

Figure 8. Hysteresis loop for Fe_3O_4 nanoparticles (upper left), Fe_3O_4/P(ODMA-VIMZ) (upper right), and Fe_3O_4/P(ODMA-VIMZ)/Au (bottom) nanocomposite particles.

polymerization reaction in order to obtain Fe_3O_4/PODMA nanocomposite particles. Three samples were prepared by varying the Fe_3O_4 content at 1, 5, and 10 wt %, respectively. Figure 5 reveals TEM images and EDS analysis of Fe_3O_4/PODMA particles with 10 wt % of encapsulated Fe_3O_4 nanoparticles.

In Figure 5(a), the larger and brighter domains show Fe_3O_4/PODMA nanocomposite particles and the smaller and dispersed domains reveal PTA used for negative staining. At higher magnifications [Figure 5(b, c)], darker domains inside the particles represent the existing encapsulated magnetite nanoparticles and it is worth mentioning that they have completely separated and are well-dispersed in the polymeric matrix inside the particles on a nanometer scale. This is a great achievement in this area because of the prevention of formation of magnetite particle aggregates. DLS analysis of the above samples shows an average particle size of 291 nm with PDI of 1.07, corresponding to what was observed from TEM micrographs.

To confirm the composition of the particles, EDS spectrum [Figure 5(d)] was collected from TEM analysis, confirming the presence of Fe ($k_\alpha = 6.4$ and $k_\beta = 7.3$ KeV) in the latex particles. As a precise verification of whether Fe_3O_4 nanoparticles have been encapsulated or exist on the surface of PODMA particles, AFM images were taken and the results are shown in Figure 6. The sample for AFM analysis was prepared by adding one drop of Fe_3O_4/PODMA latex onto the precleaned surface of a glass slide and air-dried for 24 h.

Figure 6(b, c) represents the same position of the sample at different magnifications. Figure 6(c, d) was captured at the same position and at the same magnification, but Figure 6(d) shows the phase profile of the surface of Fe_3O_4P/ODMA particles in Figure 6(c). It could be observed that the surface of Fe_3O_4/PODMA particles is quite smooth and there is no trace of adsorbed Fe_3O_4 nanoparticles on the surface of particles. This confirms that magnetite nanoparticles have been encapsulated into the PODMA particles and they tend to reside inside the polymeric phase instead of migrating towards the oil/water interface during miniemulsion polymerization.

Preparation of Fe_3O_4/PODMA/Au Nanocomposite Particles

It has been demonstrated that for an efficient reduction-deposition of Au on the surface of latex seeds, the presence of cationic surfactant plays an important role for the appropriate interaction between seed particles and $AuCl_4^-$.[55] Also, the existence of electron donating groups, which are able to establish ligation with$AuCl_4^-$ would lead to their effective adsorption on the particles' surface. Therefore, VIMZ was incorporated into the polymeric shell in the produced magnetic nanocomposite particles [Fe_3O_4/P(ODMA-*co*-VIMZ)].

Two samples with different amounts of $HAuCl_4$ were considered for the preparation of Fe_3O_4/P(ODMA-*co*-VIMZ)/Au particles (Table II). For MCG2, the concentration of Au^{3+} was two times that of MCG1 and the $NaBH_4$ concentration was kept constant for both samples. Consequently, the molar ratio between reducing agent and gold ions were set at 1 : 1.2 and 1 : 2.4 for MCG1 and MCG2, respectively. Figure 7 shows the TEM images of gold-deposited particles for the above two samples. It can be seen that the light small gold nanoparticles with particle size of

Table IV. Magnetic Parameters of the Prepared Samples by VSM Analysis

Sample	H_c (Oe)	M_r (emu/g)	M_r/M_s
Fe_3O_4	17	0.3	0.007
Fe_3O_4/P(ODMA-VIMZ)	6	0.02	0.004
Fe_3O_4/P(ODMA-VIMZ)/Au	5	0.06	0.012

H_c is coercivity, M_r is remanence, and M_s represents saturation magnetization of the particles.

10–20 nm have been deposited on the surface of the Fe_3O_4/P(ODMA-*co*-VIMZ) particles. The results reveal that the morphologies of the final particles are raspberry-like and gold nanoparticles are deposited in separate domains. Also, for the sample with higher concentration of Au^{3+} (MCG2), the density of gold nanoparticles is higher than MCG1. This gives an indication that it would be possible to adjust the density and number of Au nanoparticles in the resulting Fe_3O_4/P(ODMA-*co*-VIMZ)/Au particles by fine tuning of [Au^{3+}] in the recipe. DLS analysis of the above samples showed an average particle size of about 300 nm with PDI of 1.12.

The composition of particles was analyzed by EDS spectrum [Figure 7(c)] during TEM imaging. This spectrum confirms the presence of Fe, but for Au, because of the vicinity and overlapping of their peaks with that of W (PTA was added for negative staining), it is difficult to distinguish between them in the corresponding spectrum. Thus, we used high resolution TEM micrographs as proof for the growth of Au domains on the surface of Fe_3O_4/P(ODMA-VIMZ) seeds.

Magnetic Properties of the Particles

Magnetic properties were recorded by vibrating sample magnetometer (VSM) analysis, and Figure 8 shows the variation of magnetization with the applied magnetic field for the products obtained from each step. The results illustrate that all samples exhibit superparamagnetic properties at room temperature and encapsulation of the magnetite nanoparticles in the polymeric particles and coating with gold does not have a significant effect on their magnetic characteristics. The hysteresis loops are all S-shaped and the magnetic parameters are given in Table IV. For all samples, the ratio of remanence magnetization (M_r) to saturation magnetization (M_s) (i.e., M_r/M_s) is close to zero and illustrates the superparamagnetic properties of the products.

CONCLUSIONS

Fe_3O_4 nanoparticles were prepared in diphenyl ether as an organic media with appropriate control on the size and size distribution of the nanoparticles. These magnetite nanoparticles ($\sim$ 5 nm in size) were well dispersed in the oil phase and were encapsulated in the monomer droplets (ODMA-VIMZ) and polymerized through a miniemulsion process to obtain magnetic nanocomposite particles. The morphological studies revealed that Fe_3O_4 nanoparticles were dispersed inside the particles and did not tend to migrate toward the interface with water. Fe_3O_4/P(ODMA-*co*-VIMZ) particles were exploited as seeds for the adsorption of Au^{3+} ions. Their reduction then led to the formation of Fe_3O_4/P(ODMA-*co*-VIMZ)/Au nanocomposite particles with three different potential applications because of the simultaneous existence of magnetic properties, a polymeric layer as a matrix for loading lipophilic drugs, and gold islands with plasmonic and chemical functionalization affinities. The products from each step were characterized by TEM, EDS, and DLS analysis and magnetic properties were measured by VSM. It was found that all the samples have superparamagnetic properties and their encapsulation and gold deposition did not affect their magnetization characteristics.

ACKNOWLEDGMENTS

Ali Reza Mahdavian wishes to express his gratitude to the Iran Polymer & Petrochemical Institute for providing facilities for participation in this project at Lehigh University. Financial support from the members of the Emulsion Polymers Institute's Industrial Liaison Program is also gratefully acknowledged.

REFERENCES

1. McHenry, M. E.; Laughlin, D. E. *Acta Mater.* **2000,** *48*, 223.
2. Goon, I. Y.; Lai, L.M. H.; Lim, M.; Munroe, P.; Gooding, J. J.; Amal, R. *Chem. Mater.* **2009,** *21*, 673.
3. Robinson, D. B.; Persson, H.H. J.; Zeng, H.; Li, G.; Pourmand, N.; Sun, S.; Wang, S. X. *Langmuir* **2005,** *21*, 3096.
4. Kuznetsov, O.; Brusentsov, N.; Kuznetsov, A.; Yurchenko, N.; Osipov, N.; Bayburtskiy, F. J. *Magn. Mater.* **1999,** *194*, 83.
5. Mahdavian, A. R.; Mirrahimi, M. *Chem. Eng. J.* **2010,** *159*, 267.
6. Oliva, B. L.; Pradhan, A.; Caruntu, D.; O'Conner, C. J.; Tarr, M. A. *J. Mater. Res.* **2006,** *21*, 1312.
7. Fu, C.-M.; Wang, Y.-F.; Chao, Y.-C.; Hung, S.-H.; Yang, M.-D. *IEEE Trans. Magn.* **2004,** *40*, 3003.
8. Anzai, Y.; Blackwell, K. E.; Hirschowitz, S. L.; Rogers, J. W.; Sato, Y.; Yuh, W.T. C.; Runge, V. M.; Morris, M. R.; McLachlan, S. J.; Lufkin, R. B. *Radiology* **1994,** *192*, 709.
9. Briggs, R. W.; Wu, Z.; Mladinich, C.R. J.; Stoupis, C.; Gauger, J.; Liebig, T.; Ros, P. R.; Ballinger, J. R.; Kubilis, P. *Magn. Reson. Imaging* **1997,** *15*, 559.
10. Dobson, J. *Drug Dev. Res.* **2006,** *67*, 55.
11. Jain, T. K.; Morales, M. A.; Sahoo, S. K.; Leslie-Pelecky, D. L.; Labhasetwar, V. *Mol. Pharm.* **2005,** *2*, 194.
12. Lao, L. L.; Ramanujan, R. V. *J. Mater. Sci. Mater. Med.* **2004,** *15*, 1061.
13. Li, D.; Teoh, W. Y.; Selomulya, C.; Woodward, R. C.; Amal, R.; Rosche, B. *Chem. Mater.* **2006,** *18*, 6403.
14. Scherer, F.; Anton, M.; Schillinger, U.; Henke, J.; Bergemann, C.; Kruger, A.; Gansbacher, B.; Plank, C. *Gene Ther.* **2002,** *9*, 102.
15. Lo, C. K.; Xiao, D.; Choi, M. M. *F.J. Mater. Chem.* **2007,** *17*, 2418.
16. Gupta, A. K.; Gupta, M. *Biomaterials* **2005,** *26*, 3995.
17. Illes, E.; Tombacz, E. J. *Colloid Interface Sci.* **2006,** *295*, 115.
18. Gans, B. J.; Blom, C.; Mellema, J.; Philipse, A. P. *J. Magn. Magn. Mater.* **1999,** *201*, 11.

19. Mikhaylova, M.; Kim, D. K.; Bobrysheva, N.; Osmolowsky, M.; Semenov, V.; Tsakalakos, T.; Muhammed, M. *Langmuir,* **2004,** *20*, 2472.
20. Mandal, M.; Kundu, S.; Ghosh, S. K.; Panigrahi, S.; Sau, T.; Yusuf, S. M.; Pal, T. J. *Colloid Interface Sci.* **2005,** *286*, 187.
21. Lim, J.; Eggeman, A.; Lanni, F.; Tilton, R. D.; Majetich, S. A. *Adv. Mater.* **2008,** *20*, 1721.
22. Mykhaylyk, O.; Chernenko, A.; Ilkin, A.; Dudchenko, N.; Ruditsa, V.; Novoseletz, M.; Zozulya, Y. J. *Magn. Magn. Mater.* **2001,** *225*, 241.
23. Butterworth, M. D.; Illum, L.; Davis, S. S. *Colloids Surf. A* **2001,** *179*, 93.
24. Chatterjee, J.; Haik, Y.; Chen, C. J. *J. Magn. Magn. Mater.* **2002,** *246*, 382.
25. Pardoe, H.; Chua-Anusorn, W.; St. Pierre, T. G.; Dobson, J. J. *Magn. Magn. Mater.* **2001,** *225*, 41.
26. Zhang, Z. J.; Wang, Z. L.; Chakoumakos, B. C.; Yin, J. S. *J. Am. Chem. Soc.* **1998,** *120*, 1800.
27. Neveu, S.; Bec, A.; Robineau, M.; Talbol, D. J. *Colloid Interface Sci.* **2002,** *255*, 293.
28. Pileni, M. P.; Moumen, N. J. *Phys. Chem. B* **1996,** *100*, 1867.
29. Liu, C.; Zou, B.; Rondinone, A. J.; Zhang, Z. J. *J. Phys. Chem. B* **2000,** *104*, 1141.
30. Sun, S.; Zeng, H.; Robinson, D. B.; Raoux, S.; Rice, P. M.; Wang, S. X.; Li, G. J. *Am. Chem. Soc.* **2004,** *126*, 273.
31. Hyeon, T.; Lee, S. S.; Park, J.; Chung, Y.; Na, H. B. *J. Am. Chem. Soc.* **2001,** *123*, 12798.
32. Guo, Q.; Teng, X.; Rahman, S.; Yang, H. J. *Am. Chem. Soc.* **2003,** *125*, 630.
33. Redl, F. X.; Cho, K.-S.; Murray, C. B.; O'Brien, S. *Nature* **2003,** *423*, 968.
34. Sun, S.; Zeng, H. J. *Am. Chem. Soc.* **2002,** *124*, 8204.
35. Wang, L.; Luo, J.; Fan, Q.; Suzuki, M.; Suzuki, I. S.; Engelhard, M. H.; Lin, Y.; Kim, N.; Wang, J. Q.; Zhong, C.-J.J. *Phys. Chem. B* **2005,** *109*, 21593.
36. Caruntu, D.; Remond, Y.; Chou, N. H.; Jun, M.-J.; Caruntu, G.; He, J.; Goloverda, G.; O'Conner, C. J.; Kolesnichenko, V. L. *Inorg. Chem.* **2002,** *41*, 6137.
37. Caruntu, D.; Caruntu, G.; Chen, Y.; O'Conner, C. J.; Goloverda, G.; Kolesnichenko, V. L. *Chem. Mater.* **2004,** *16*, 5527.
38. Lyon, J. L.; Fleming, D. A.; Stone, B. B.; Schiffer, P.; Williams, M. E. *Nano Lett.* **2004,** *4*, 719.
39. Wang, L.; Luo, J. M.; Maye, M. M.; Fan, Q.; Rendeng, Q.; Engelhard, M. H.; Wang, C.; Lin, Y.; Zhong, C.-J.J. *Mater. Chem.* **2005,** *15*, 1821.
40. Xu, Z.; Hou, Y.; Sun, S. J. *Am. Chem. Soc.* **2007,** *129*, 8698.
41. Lee, Y.; Lee, J.; Bae, C. J.; Park, J. G.; Noh, H. J.; Park, J. H.; Hyeon, T. *Adv. Funct. Mater.* **2005,** *15*, 503.
42. Hsiao, S.-C.; Ou, J.-L.; Sung, Y.; Chang, C.-P.; Ger, M.-D. *Colloid Polym. Sci.* **2010,** *288*, 787.
43. Sudol, E. D.; El-Aasser, M. S. In Emulsion Polymers and Emulsion Polymerization; Lovell, P. A.; El-Aasser, M. S., Eds.; Wiley and Sons: England, **1997;** Chapter 20, p 700.
44. El-Aasser, M. S.; Sudol, E. D. *J. Coat. Technol. Res.* **2004,** *1*, 21.
45. Erdem, B.; Sudol, E. D.; Dimonie, V. L.; El-Aasser, M. S. *J. Polym. Sci. A: Polym. Chem.* **2000,** *38*, 4419.
46. Erdem, B.; Sudol, E. D.; Dimonie, V. L.; El-Aasser, M. S. *J. Polym. Sci. A: Polym. Chem.* **2000,** *38*, 4431.
47. Erdem, B.; Sudol, E. D.; Dimonie, V. L.; El-Aasser, M. S. *J. Polym. Sci. A: Polym. Chem.* **2000,** *38*, 4441.
48. Erdem, B.; Sudol, E. D.; Dimonie, V. L.; El-Aasser, M. S. *Macromol. Symp.* **2000,** *155*, 181.
49. Mahdavian, A. R.; Ashjari, M.; Salehi-Mobarakeh, H. J. *Appl. Polym. Sci.* **2008,** *110*, 1242.
50. Mahdavian, A. R.; Sehri, Y.; Salehi-Mobarakeh, H. *Eur. Polym. J.* **2008,** *44*, 2482.
51. Choi, Y. T.; Sudol, E. D.; Vanderhoff, J. W.; El-Aasser, M. S. J. Polym. Sci. Polym. Chem. Ed. **1985,** *23*, 2973.
52. Miller, C. M.; Sudol, E. D.; Silebi, C. A.; El-Aasser, M. S. *Macromolecules* **1995,** *28*, 2765.
53. Landfester, K.; Bochthhold, N.; Foster, S.; Antinietti, M. *Macromol. Rapid Commun.* **1999,** *20*, 81.
54. Csetneki, I.; Faix, M. K.; Szilagyi, A.; Kovacs, A. L.; Nemeth, Z.; Zrinyi, M. J. *Polym. Sci. A: Polym. Chem.* **2004,** *42*, 4802.
55. Kim, H.; Daniels, E. S.; Dimonie, V. L.; Klein, A. J. *Polym. Sci. A: Polym. Chem.* **2008,** *46*, 912.
56. Hong, R. Y.; Pan, T. T.; Han, Y. P.; Li, H. Z.; Ding, J.; Han, S. J. *J. Magn. Magn. Mater.* **2007,** *310*, 37.
57. http://www.chemicaldictionary.org, **2009.**
58. Casey, M. B.;Sudol, E. D.; El-Aasser, M. S. PMSE Preprints, Vol. 99, 236th ACS National Meeting, Philadelphia, PA, August 17–21, **2008.**
59. Brandrup, J.; Immergut, E. H. In Polymer Handbook, 3rd ed.; Wiley-Interscience: USA, **1989.**